Uptake of phosphorus by epilithon in three oligo- to mesotrophic post-mining lakes

Eliška Konopáčová (eliska.konopacova@hbu.cas.cz)
University of Pardubice
Jiří Nedoma
Biology Centre
Kateřina Čapková
Biology Centre
Petr Čapek
University of South Bohemia
Petr Znachor
Biology Centre
Miloslav Pouzar
University of Pardubice
Milan Říha
Biology Centre
Klára Řeháková
Biology Centre

Research Article

Keywords: mesotrophic post-mining lakes, epilithon, phosphorus (P) cycling

Posted Date: March 18th, 2021

DOI: https://doi.org/10.21203/rs.3.rs-319967/v1

Uptake of phosphorus by epilithon in three oligo- to mesotrophic post-mining lakes

Eliška Konopáčová[1, 2*], Jiří Nedoma[2], Kateřina Čapková[2], Petr Čapek[4], Petr Znachor[2,4], Miloslav Pouzar[1, 3], Milan Říha[2] & Klára Řeháková[2]

[1]Institute of Environmental and Chemical Engineering, Faculty of Chemical Technology, University of Pardubice, Studentská 573, 530 12 Pardubice, the Czech Republic, [2]Institute of Hydrobiology, Biology Centre v.v.i., Czech Academy of Sciences, Na Sádkách 702/7, 370 05 České Budějovice, the Czech Republic, [3]Center of Materials and Nanotechnologies (CEMNAT), University of Pardubice, Nám. Čs. Legií 565, 530 02 Pardubice, the Czech Republic, [4]University of South Bohemia, Faculty of Sciences, Branišovská 1645/31A, 370 05 České Budějovice, the Czech Republic, *email: eliska.konopacova@hbu.cas.cz

Abstract

Epilithon contributes to phosphorus (P) cycling in lakes, but its P uptake traits have been rarely studied. We measured the chemical composition of epilithon and its inorganic P uptake kinetics using isotope ^{33}P in three deep oligo- to mesotrophic post-mining lakes in April, July, and October 2019. Over the sampling period, epilithon biomass doubled, while the P content in biomass dropped to 60% of the April values. High epilithic C:P molar ratios (677 on average) suggested strong P deficiency in all investigated lakes.

Regarding the kinetic parameters of phosphorus uptake, maximum uptake velocity (V_{max}, seasonal range 0.9–101 mg P g OM^{-1} h^{-1}) decreased by an order of magnitude from April to October, while half-saturation constant (K_S, 1.6–103 mg P L^{-1}) did not show any consistent temporal trend. We found a general decrease in the specific P uptake affinity (0.1–2.2 L g OM^{-1} h^{-1}) and the estimated *in-situ* P uptake (0.04–2.3 µg P g OM^{-1} h^{-1}) of epilithon over the season, which might have resulted from changes in epilithon community composition, a decreasing ratio of living biomass to extracellular polymers and detritus, rapid internal recycling, and/or thickening of the epilithic biofilm. Additionally, we observed a phenomenon of reversible abiotic P adsorption on epilithon.

Introduction

Periphyton is an assemblage of autotrophic and heterotrophic organisms that produces extracellular polymeric substances, all together forming a biofilm attached to a solid substrate[1,2]. Epilithon is a subgroup of periphyton covering submerged surfaces of stones[1]. Periphyton represents an important component of aquatic food webs and biodiversity[1,3] and can contribute considerably to nutrient cycling[4,5]. Along with phytoplankton and submerged macrophytes, periphyton can account for up to 92% of the total primary production in oligotrophic lakes[6].

Periphyton productivity may be limited by the availability of inorganic nutrients, especially phosphorus (P). Phosphorus is an essential constituent of microbial cells. Integrated into phospholipids, nucleic acids, coenzymes and various metabolites, it is considered the most common element limiting the growth rates and metabolic activities of photoautotrophs in temperate freshwater ecosystems[7,8]. Whereas P uptake by phytoplankton has been widely studied[9–12], only few studies have addressed the kinetics of P uptake by periphyton in lentic waters[13,14] and no study ever quantified the P uptake of periphyton in temperate freshwaters. Given the above-mentioned importance of periphyton for total primary production of lakes, the periphyton P uptake might be significant as well. A study of P fluxes in the shallow subtropical Lake Okeechobee found a significantly greater P uptake in phytoplankton than in periphyton. However, in an oligotrophic marsh area in the lake, due to the well-developed periphytic biomass, the cumulative P uptake by periphyton was twice as high as P uptake by phytoplankton[14].

A thorough analysis of periphyton and phytoplankton contributions to P cycling in lake ecosystems requires the determination of kinetic parameters of P uptake for both periphyton and phytoplankton. In osmotrophic organisms, phosphorus can only be taken up

in substantial amount in the form of inorganic orthophosphate (P_i)[15]. The relationship between P_i concentration in water and its uptake rate can be often described by a hyperbolic function analogous to Michaelis-Menten equation for enzymatic reaction kinetics possessing two parameters: maximum velocity (V_{max}) and half-saturation constant (K_S, concentration at which V_{max} = 1/2). However, at extremely low P_i concentrations, typical for oligotrophic waters, P uptake velocity is far below V_{max}, as P_i is much smaller than K_S[16,17]. A relevant parameter describing P uptake and the competitive ability of microorganisms at low P_i is the specific P uptake affinity (*SPUA*), calculated as a proportion of V_{max} and K_S, equal to the initial slope of the function at the beginning of the curve[18,19]. Interpretation of the *SPUA* values is not straightforward due to their unusual units (L mg OM^{-1} h^{-1}); however, it is analogous to the clearance rate of zooplankton – the volume of water cleared of phosphate per unit biomass per unit time[20].

Large lakes newly emerge during the hydric recultivation of post-mining pits. Understanding the nutrient cycling and energy fluxes in the unique ecosystems of post-mining lakes is urgently needed since their number is expected to rise in the upcoming decades due to the coal mining suppression associated with the European Union's Green Deal[21,22]. Post-mining lakes are often oligotrophic with very low P concentrations (total phosphorus, *TP* < 15 µg L^{-1} and soluble reactive phosphorus concentration, *SRP* ~1 µg L^{-1})[23]. However, no detailed report on P cycling in these lakes and about the organisms involved is available.

In the present study we sampled three recently flooded oligo- to mesotrophic post-mining lakes in the north-west region of the Czech Republic (Milada, Medard and Most Lakes) to evaluate the role of dissolved inorganic phosphorus acquisition for periphyton nutrition and in-lake nutrient cycling. Despite very low P concentration in water, dense mats

77 of periphyton, mainly represented by epilithon, have developed in all investigated lakes
78 (Řeháková, unpublished data).
79 We sought to investigate P uptake traits of epilithon in these three lakes during the
80 whole vegetation season, using ^{33}P-labelled orthophosphate. Our specific objectives were (i)
81 to determine kinetic parameters of the epilithon P uptake, namely the specific P uptake
82 affinity ($SPUA_E$), maximum P uptake velocity ($V_{max,}$), and half-saturation constant (K_S); (ii) to
83 estimate *in-situ* P uptake by epilithon; (iii) to decipher the environmental factors affecting
84 the specific P uptake affinity; and (iv) to compare specific P uptake affinities of epilithon and
85 phytoplankton.

Results

Background limnological parameters

All lakes (see **Fig. 1** for their geographic position) had high water transparency corresponding to the euphotic depth (the depth of 1% of the surface irradiance) between 10 and 18 m (**Table 1**) and were stratified with the mixed depth varying from 3 to 11 m. In April, the sampling was performed shortly after the spring overturn, thus the stratification was weak, nutrient concentrations were higher, and the temperature lower (7–11 °C), than in summer and autumn (13–24 °C, **Table 1**). Lakes Medard and Most were characterised by a low chlorophyll *a* (*Chla*) and total phosphorus (*TP*) concentrations (0.9 and 1.9 µg L^{-1}; 4.2 and 11 µg L^{-1} respectively in their seasonal averages). Lake Milada's *Chla* and *TP* concentrations were slightly higher (5.1 and 14.1 µg L^{-1}, respectively).

Epilithon characterisation

Parameters related to epilithon biomass and chemical composition, as well as their differences among lakes and seasonal development with statistical differences are summarised in **Fig. 2** and in **Table 2** (for the full two-way ANOVA table see **Supplementary Table 1**). Epilithon biomass expressed as organic matter (*OM*) content and normalised per area on average doubled from April (1.8 mg cm^{-2}) to October (3.6 mg cm^{-2}), being about three times higher in Lake Milada (4.8 mg cm^{-2}) than in the two other lakes (**Table 2, Fig. 2a**); the corresponding dry-weight figures showed a similar pattern (**Table 2, Fig. 2a**). Average biomass P content dropped from 3.6 mg P g OM^{-1} in April to 2.2 mg P g OM^{-1} in October independently of the lake (**Table 2**). In contrast, average epilithic P content per area considerably differed among the lakes, being 2.5 times higher in Milada Lake (11 µg P cm^{-2})

than in the two other lakes and showing contrasting seasonal trends - a decrease in Most Lake and an increase in the other lakes.

Epilithon nutrient molar element ratios were generally high (**Table 2**) - C:P ratios ranged from 160 to 1260, N:P ratios ranged from 13 to 68 (**Fig. 2b**), and C:N ratios ranged from 12 to 25 (**Fig. 2c**), being on average 1.3–2.0 times lower in Lake Medard than in the two other lakes (**Table 2**, **Fig. 2b,c**). All the ratios were significantly (up to 2-fold) higher in June and October than in April (**Table 2**, **Fig. 2b, c**).

Epilithon P uptake - laboratory measurements

There was no systematic variability in any epilithon P uptake parameter within lakes (north shore vs. south shore; a depth of 0.5 m vs. 1.5 m; paired t-tests, p = 0.12–0.81). Hence, all these in-lake values were treated as replicates (n = 4, see, e.g., **Figs. 3–5**). Time course data on P uptake by epilithon (i.e. ^{33}P disappearance from water) were fitted well to a simple monoexponential model (**Supplementary Fig. 1, Supplementary Table 2**). Fourteen out of the 348 progress curves were excluded due to a lack of fit (high scatter or an increasing trend in the data). Calculated P uptake velocities (v_{upt}) varied widely from 0.04 to 112 mg P g OM^{-1} h^{-1} and were strongly concentration-dependent (**Supplementary Table 2**). The relationship between v_{upt} and P_{add} followed the Michaelis-Menten kinetics in 28 out of the 35 cases, while the remaining seven followed the simplified linear model (**Table 3, Supplementary Figs. 2–4**). Maximum P uptake velocity (V_{max}) ranged between 0.9–101 mg P g OM^{-1} h^{-1}. The corresponding estimates of the half-saturation constant (K_S) ranged from 1.6 to 103 mg P L^{-1} (**Table 3, Fig. 3b, c**). Both V_{max} and K_S significantly decreased over the season by around one order of magnitude, while the observed differences among lakes became less prominent and were statistically significant only for V_{max} (**Table 2, Fig. 3b, c**).

The specific P uptake affinity of epilithon ($SPUA_E$), representing the initial slope of the v_{upt} vs. P_{add} plot, ranged from 0.11 to 2.22 L g OM^{-1} h^{-1} (**Table 3**, **Fig. 4a**). There was a significant seasonal decrease in $SPUA_E$ from 1.3 to 0.37 L g OM^{-1} h^{-1} independently of the lake (**Table 2**). The generalised linear mixed-effect model with season and lake treated as random factors indicated the C:N molar ratio of the epilithon biomass ($p < 0.001$) and the lake-water pH ($p < 0.002$) as significant drivers of $SPUA_E$.

All values of P uptake parameters reported throughout this paper have not been corrected for abiotic P uptake (see Discussion). Abiotic ^{33}P adsorption occurring in the presence of 4-% formaldehyde was relatively high, accounting on average for 8% (range 1–18%), 24% (7–61%), and 54% (21–90%) of the formaldehyde-untreated samples in Lakes Milada, Most and Medard, respectively (**Fig. 3a**). In three additional experiments, we applied formaldehyde at a wide range of P concentrations (0.1–10 mg P L^{-1}). In two of those we observed a roughly two-fold increase in P adsorption with increasing P concentration, whereas no concentration dependence was found in the remaining experiment (**Supplementary Fig. 5**). We discovered that more than one half of the adsorbed P (50–70%) could be readily released back to the dissolved phase during a one-hour treatment of the samples with an oxalacetate-based "surface wash reagent" (**Supplementary Table 3**), which indicates a weak and reversible abiotic P adsorption.

Epilithon P uptake - calculated *in-situ* P dynamics

In-situ epilithon P uptake velocities (*EPUV*, µg P g OM^{-1} h^{-1}) calculated from the specific P uptake affinity and SRP_{corr} (corrected soluble reactive phosphorus concentration, see Methods for explanation) were rather low and variable (0.04 to 2.3 µg P g OM^{-1} h^{-1}). On

156 average, the *in-situ* epilithon P uptake was roughly twice as high in Lake Most compared to
157 the other lakes, with a generally decreasing seasonal trend (**Table 2, Fig. 4b**).
158 Epilithon P doubling time (*EPDT*) – i.e. the theoretical time necessary for doubling the
159 actual P content in the biomass assuming the *in-situ* P uptake velocity estimated as above –
160 ranged from 30 to 3,940 days (**Fig. 5a**). Average *EPDT* increased over the season from 140
161 days in April to 800 days in October. In Lake Medard, it was three to four times as high as in
162 Lakes Most and Milada (800 days vs. 200–300 days, respectively; **Table 2**, **Fig. 5a**).
163 Finally, theoretical amounts of the P that epilithon could have sequestered from the
164 water column during the periods between the two successive sampling campaigns were
165 calculated (63–105 days) assuming the estimated *in-situ* P uptake velocity. These theoretical
166 values were compared with observed changes in P content determined in the biomass (**Fig.**
167 **5b**). The observed and the calculated changes in the epilithon P content did not differ
168 statistically in Lakes Milada and Medard. In contrast, the theoretical values greatly exceeded
169 the observed ones in Lake Most, where a decrease or minor change in the P content was
170 measured (**Fig. 5b**).
171
172 Seston P dynamics and comparison with epilithon
173 Turnover time of dissolved orthophosphate measured with ^{33}P ranged from 7 minutes
174 to 3.6 hours indicating moderate (in spring) to extreme (in summer and autumn) P deficiency
175 in all lakes (**Supplementary Table 5**). Seston P uptake kinetics followed the Michaelis-
176 Menten model (**Supplementary Fig. 6**), yielding V_{max} estimates ranging from 0.29 to 1.3 µg P
177 L^{-1} h^{-1} and K_S from 0.4 to 6.1 µg P L^{-1} (**Supplementary Table 5**)**.** The specific P uptake
178 affinities in seston ranged from 230 to 24,000 L g OM^{-1} h^{-1}, being thus 2–4 orders of

magnitude higher (**Supplementary Table 5**) than the epilithon-specific values (0.11–2.22 L g OM^{-1} h^{-1}, **Table 3**).

Discussion

Data on periphyton P uptake kinetics in lentic systems are extremely scarce in the literature[13,14,24]. Our study represents the first report on P uptake kinetics by epilithon assemblages naturally growing on stones in temperate oligo- to mesotrophic lakes. The only comparable data are available from very different freshwater habitats (a subtropical lake and wetlands)[13,14]. The values of specific P uptake affinity ($SPUA_E$) measured in this study (0.11–2.22 L g OM^{-1} h^{-1}) were roughly one order of magnitude lower than those presented for periphyton by Scinto and Reddy in subtropical wetlands[13]. While V_{max} estimates presented in our study (0.9–101 mg P g OM^{-1} h^{-1}) roughly match the values available in the literature, our K_S estimates (1.6–103 mg P L^{-1}) are 1–3 orders of magnitude higher than those previously reported[13,14]. The among-system differences in kinetic parameters might be attributed to the differences in abiotic and biotic drivers affecting P uptake in compared ecosystems, in the species composition of periphyton, environmental conditions, and morphological and limnological variances between studied lakes. In freshwater wetlands, extreme periphytic N:P ratios (152–231) have been reported[13]. Such high values suggest a strong P limitation of these wetlands and may explain the ten times higher $SPUA_E$ compared to our estimates. A positive relationship between the degree of P deficiency and $SPUA_E$ is well documented in algae[10,25]. The wide range of linear increase in P uptake velocity with concentration of dissolved P, reflected by high K_S values or even by the absence of saturation, might represent an adaptation of the epilithon community to episodic increases or pulses of dissolved P, ensuring optimal utilisation of available resources.

Variability in $SPUA_E$ was statistically related to both epilithon C:N molar ratio and lake-water pH. The negative relation between $SPUA_E$ and epilithon C:N could indicate a tendency to a decrease in specific P uptake affinity under conditions of N+P co-limitation of the

205 epilithic microbial community[26]. Notably, the highest epilithon C:N ratios (around 22) were
206 observed at Lake Milada in July and October (**Fig. 2c**), concomitantly with low $SPUA_E$ values
207 (**Fig. 4a**) and an extremely low lake-water nitrate concentration (0.02 mg L^{-1}; **Table 1**),
208 generally considered to be limiting for algal growth[27]. Since the naturally growing epilithon
209 consist of a variety of species, some of them might have been N-limited, whereas the others
210 might have been P-limited. Following this logic, this could have led to a lower P demand and
211 lower $SPUA_E$ values of the epilithic community. However, the relation of $SPUA_E$ to species
212 composition, was not a subject of this study. The relationship between $SPUA_E$ and *pH*
213 remains rather obscure.
214 In the lakes studied, epilithon biomass per area and nutrient stoichiometry
215 corresponded with the values reported for comparable oligotrophic lakes[28]. Two slightly
216 different stoichiometric definitions of growth-limiting conditions were suggested in the
217 literature. According to Hillebrand and Sommer, P limitation of benthic algae is indicated
218 when C:P > 180 and N:P > 22[26]. Kahlert reported the threshold for P limitation of periphyton
219 when C:P > 369 and N:P > 32[29]. Applying both definitions, the values found in the
220 investigated post-mining lakes (average C:P 680 and N:P 39) indicate P limitation of epilithic
221 growth which tends to strengthen over the season (**Fig. 2b**). A comparably high epilithic C:P
222 and N:P ratios were reported also for deep oligotrophic lakes in Sweden (C:P and N:P ratios
223 up to 800 and 74, respectively)[28] and an oligotrophic lake in north-western Ontario (C:P ratio
224 820)[30].
225 We observed a discrepancy between the seasonal development of $SPUA_E$ and of the
226 other P limitation indices. Epilithon biomass cover (OM per cm^2) roughly doubled, while
227 biomass P content roughly halved from April to July and October. One would expect a
228 simultaneous increase in $SPUA_E$ in response to strengthened P limitation[10,25] implied by an

observed decrease in P content and increase in C:P ratio. However, the opposite was found, i.e. $SPUA_E$ decreased roughly ten times during the same period (**Table 2, Fig. 4a**). There are several possible explanations for this apparent contradiction: (1) Seasonal changes in the epilithic microbial community might favour species with lower P requirements: Seasonal shifts in the phototrophic assemblage composition were in fact observed; however, the significance of their relationship with $SPUA_E$ has not been proven(Řeháková et al. in prep.). It has been reported in the literature that higher periphyton C:P ratios can be associated with shifts towards a higher contribution of heterotrophic over autotrophic organisms[31]. (2) The decreasing ratio of living biomass to structural (mainly extracellular) polymers or detritus during the seasonal succession: $SPUA_E$ was normalised to the total *OM* content, thus including both living and dead cells as well as extracellular polymeric substances. This explanation appears to be supported by the facts that the C:P ratio doubled from spring (~410) to the extreme values in summer and autumn (~820, **Fig. 2b)**. (3) The high efficiency of P internal recycling in epilithon. P released out from the dying biomass may be taken up by the living cells in the epilithon without leaving the biofilm thus lowering the demand for external P input. (4) The decreased accessibility of P to epilithic microorganisms due to the thickening of the epilithic biofilm on the stone over the season: If true, this would markedly constrain P diffusion through the epilithon matrix as described by Riber and Wetzel[32]. As a result, the cells situated closer to the stone substrate could exhibit lower P uptake than the cells situated near the surface of the biofilm even if their individual P uptake affinities were high. Consequently, this would lead to lower values of overall P uptake and of the related parameters ($SPUA_E$, V_{max} *etc*.) of the epilithon.

In-situ epilithon P uptake velocities were calculated by multiplying $SPUA_E$ by the corrected soluble reactive phosphorus values, SRP_{corr} to elucidate how much our kinetic

measurement of P uptake by epilithon can explain the changes in epilithic P content that actually occurred between sampling campaigns. Although the calculated *in-situ* P uptake velocities were extremely low, the observed and calculated (potential) changes in epilithon P content were roughly in agreement in Lakes Milada and Medard. However, in Lake Most, where epilithon P uptake velocity was the highest, the calculated changes greatly exceeded the observed ones (**Fig. 5b**), indicating high community losses due to e.g. fragile parts removal, disturbances[33], intensive grazing[34] or parasite-induced cell lysis[35].

Our *in-situ* P uptake calculations suffer from an important but unavoidable limitation: generally, P_i concentrations in the lake-water cannot be reliably determined under P limiting conditions because of their extremely low values[9]. *In-situ* epilithon P uptake velocities were calculated by multiplying the $SPUA_E$ values by SRP_{corr} (Eq. 7). The calculation is only plausible if SRP_{corr} is a reliable estimate of P_i concentration, which is extremely unlikely as the correction relies on *SRP* concentration determined with molybdenum blue method[36] known to highly (up to 100 times) overestimate the actual P_i concentration at low *SRP* levels (< 5 µg P L^{-1}) due to the interference with arsenates and hydrolysed organic phosphorus[9]. One possibility how to approach the actual P_i concentration would be an application of the radiobioassay suggested by Rigler[37]. However, the assay is biased by a subjective decision. Instead, the conservative correction was used, which is unambiguous (Eq. 7) and based on the fact that P_i concentration in lake water cannot exceed $K_S sest$ estimated by measurement of saturation kinetics of sestonic P uptake if the experiment is carried out in the presence of P_i naturally occurring in the water sample[38]. The values of SRP_{corr}, however, still represent only the upper limit of the real P_i concentration in lake water and consequently also the estimates of any derived parameters are on their upper limits.

Our values of epilithic specific P uptake affinity, $SPUA_E$, were 2–4 orders of magnitude lower than the corresponding values for seston, $SPUA_{sest}$ (**Supplementary Table 5**). Similar differences were also reported for a shallow subtropical lake in Florida[14]. The differences between $SPUA_{sest}$ and $SPUA_E$ likely result from the mostly unicellular arrangement of sestonic bacterio- and phytoplankton that tends to maximise surface to volume ratio[39], while epilithic P uptake is affected by a limited surface for nutrients entering the biofilm and the presence of an extracellular matrix that limits their transport from water into the cells[32,40].

The use of naturally growing epilithon assemblage in the present study is challenging, yet provides more ecologically relevant data compared to the commonly used artificial substrates[41,42]. An obvious disadvantage is, however, an inherent heterogeneity of individual samples, resulting in a high scatter of P uptake data (see **Supplementary Figs. 2–4**). The average difference in duplicates was 30%, but the differences were frequently several-fold. Nevertheless, variation coefficients of $SPUA_E$ and V_{max} estimates were on average 23% (range 7–55%) and 25% (range 8–47%), respectively, (**Table 3**), documenting that these P-uptake-related kinetic parameters were measured with acceptable error. The estimates of K_S were, however, less reliable (on average 44% with range 15–80%).

Values of P uptake parameters reported throughout this paper have not been corrected for abiotic P uptake (i.e. uptake occurring in the presence of 4% formaldehyde), since the results of abiotic adsorption experiments were inconclusive, showing variable concentration dependency of the formaldehyde effect (**Supplementary Fig. 5**), which does not allow P uptake to be corrected properly. Nevertheless, the abiotic P uptake was substantial, averaging at 54% of total P uptake in Lake Medard, 24% in Lake Most, and 8% in Lake Milada (**Fig. 4B)**. In additional experiments, oxalate-based surface wash reagent released 50–70% of such abiotically adsorbed P, indicating a weak and reversible P binding.

300 (**Supplementary Table 3**). Similarly, Sañudo-Wilhelmy et al. reported surface abiotic P
301 adsorption ranging from 60 to 90% of the apparent total P uptake in the phytoplankton[43].
302 Surface P adsorption has been suggested to be a mechanism for storing the temporary
303 excess of P before it can be transported into the algal cells[44]. Our data indicate that the
304 phenomenon of temporary abiotic P adsorption could be important also in periphyton, but
305 so far this has not been considered and thus requires further attention in both theoretical
306 and experimental studies.

Methods

Study sites

Three oligo- to mesotrophic post-mining lakes, Milada (area: 252 ha, max/average depth: 25/16 m, flooded in 2010), Medard (493 ha, 59/28 m, flooded in 2016), and Most (311 ha, 75/22 m, flooded in 2014), situated in the northwestern Bohemia, the Czech Republic, were chosen as study sites (**Fig. 1, Supplementary Figs. 7–9**). All lakes possess well-developed epilithon assemblages in their littoral zone (**Supplementary Fig. 10**). Basic limnological parameters of the lakes are summarised in **Table 2**.

Sampling

In each lake, epilithon was sampled at two opposite shores of each lake, designated as North (N) and South (S) (see **Fig. 1** and **Supplementary Table 6** for more details). Twelve small epilithon-covered stones (approx. diameter 4 cm) were gently collected by scuba diving at each site from 0.5 and 1.5 m depths in April, July, and October 2019. Lake water for chemical analyses and epilithon P uptake experiments was collected with a Friedinger sampler above the deepest points of the lakes from the depth of 0.5 m. Epilithon samples were kept in the lake water at *in-situ* temperature and a photoperiod of 16:8 (light:dark) until the P uptake experiments (< 2 days). The cell-free filtrate of lake water was prepared by passing it through a PCTE filter (0.22-µm porosity; Sterlitech Corporation, Seattle, USA) and stored at 4 °C until the start of the experiment (< 2 days).

Background limnological parameters

Vertical profiles of water temperature, pH, and O_2 concentration were measured with YSI EXO 2 multiparametric probe (YSI Inc., Yellow Springs, USA). The euphotic depth was

331 estimated as the depth of 1 % of surface irradiance calculated from vertical light profiles
332 obtained using LICOR LI-1400 datalogger with a spherical quantum underwater sensor LI 193
333 SA (Licor, Lincoln, NE, USA). Chlorophyll a (*Chla*) was determined according to ISO
334 10260:1992[45], total organic carbon (*TOC*) and total nitrogen (*TN*) were determined using
335 Shimadzu *TOC/TN* analyser. Total phosphorus (*TP*) was measured spectrophotometrically
336 after nitric-perchloric acid digestion[46] using Flow Injection Analyser. Dissolved reactive silica
337 (*DSi*)[47] and soluble reactive phosphorus (*SRP*)[36] were determined spectrophotometrically.
338 Nitrate-nitrogen (NO_3-*N*) was determined following the procedure of Procházková[48].
339
340 Epilithon chemical characterisation
341 After termination of ^{33}P uptake experiments (see below), epilithon was quantitatively
342 removed from each stone, dried at 110°C to constant weight and the dry weight (*DW*) was
343 determined. To determine the organic matter (*OM*) content, the dry sample was combusted
344 in a muffle furnace at 450°C for 12 h. For determination of epilithon elemental (C, N, P)
345 composition and biomass (*DW* and *OM* per area), we used different stones than those used
346 for uptake experiments, albeit collected from the same sampling site. Samples were frozen
347 till the analysis at –20 °C and homogenised using glass beads and an automatic homogeniser.
348 *TN*, *TOC*, and *TP* were analysed, as described above.
349
350 Epilithon P uptake kinetics
351 Before each experiment, the lake water was removed from containers containing
352 epilithon-covered stones. Stones were gently rinsed with 50 mL of the 0.2-µm filtered (cell-
353 free) lake water, and 100 mL of the filtered water was added. The containers were
354 supplemented with five different concentrations of orthophosphate (P_{add}, 1, 3, 10, 30, 100

mg P L^{-1}, added as KH_2PO_4) in duplicates. Incubations started by the addition of carrier-free ^{33}P-labelled H_3PO_4 (50–100 kBq; American Radiolabelled Chemicals, Inc., St. Louis, USA) along with unlabelled orthophosphate into testing containers placed in a gently shaken (120 rev/min) water bath tempered at *in-situ* temperature. Samples were incubated for 180–240 min under laboratory illumination (cca 10 µE m^{-2} s^{-1} PAR). At 15–30 min intervals, 0.6-mL aliquots were transferred into Eppendorf tubes containing 0.6 mL of scintillation cocktail (Packard Ultima Gold) and vortexed vigorously. Radioactivity (typically 20–40 thousand c.p.m. per aliquot) was determined with a liquid scintillation counter (Tri-Carb 2900TR, Packard, USA). Control for abiotic uptake was performed by adding formaldehyde (final concentration of 4%) into two containers (P_{add} = 1 mg P L^{-1}) overnight before an experiment.

P incorporation into the epilithon biomass was considered to be proportional to the ^{33}P disappearance from incubation water, as confirmed in an experiment with simultaneous spectrophotometric and scintillation detection of dissolved P (not shown). The P uptake rate constant, k_{upt} (h^{-1}), which reflects the initial uptake rate, was calculated using the two-parameter exponential function:

$$A_t = A_0 \times e^{(-k_{upt} \times t)}, \quad (1)$$

where t (hours) is time and A_t and A_0 are ^{33}P activities (c.p.m.) at the time t and zero, respectively. The velocity of P uptake by epilithon, v_{upt} (mg P g OM^{-1} h^{-1}) was calculated as:

$$v_{upt} = \frac{k_{upt} \times P_{add} \times V_{inc}}{OM}, \quad (2)$$

where V_{inc} (L) is incubation volume, and OM (g) is organic matter content in the epilithon sample. To study concentration dependence of the P uptake velocity, it was plotted as a function of P_{add} and fitted either to a Michaelis-Menten model:

$$v_{upt} = \frac{V_{max} \times P_{add}}{K_S + P_{add}}, \quad (3)$$

or, if the P uptake velocity did not show saturation, to a simplified linear model:

$$v_{upt} = v_{slope} \times P_{add}, \quad (4)$$

where V_{max} (the maximum P uptake velocity; mg P g OM^{-1} h^{-1}) and K_S (half-saturation constant; mg P L^{-1}) are the parameters of the Michaelis-Menten model (Eq. 3); the linear model (Eq. 4) had only one parameter, $v_{slope,}$ (L g OM^{-1} h^{-1}). The more complex model (Eq. 3) was selected in preference to the simpler one (Eq. 4) when improving the fit at the probability level of $p<0.05$ (F test). Parameter estimations and model selection were performed in PRISM v.7 (GraphPad Software). For saturation data (Eqs. 3, 4), relative weighting by $1/(v_{upt})^2$ was applied as the error of the v_{upt} was heteroscedastic, accounting for around 30% (average difference between duplicates), irrespectively of P_{add}. No weighting was applied to the time-course data. Outliers were excluded with the PRISM v.7 built-in algorithm using the recommended settings[49].

Epilithon specific P uptake affinity, $SPUA_E$ (L g OM^{-1} h^{-1}) for the Michaelis-Menten model (Eq. 3) was calculated as:

$$SPUA_E = V_{max}/K_S, \quad (5)$$

while for the linear model (Eq. 4) it was directly equal to v_{slope}. To estimate *in-situ* epilithon P uptake velocity (*EPUV*, µg P g OM^{-1} h^{-1}), $SPUA_E$ was multiplied with SRP_{corr} (corrected soluble reactive phosphorus concentration; µg P L^{-1}):

$$EPUV = SPUA_E \times SRP_{corr}, \quad (6)$$

where SRP_{corr} is:

$$SRP_{corr} = \min(SRP, K_S sest). \quad (7)$$

As Eq. 7 suggests, SRP_{corr} was defined as directly measured *SRP* when $SRP < K_S sest$. Vice versa, where $SRP > K_S sest$, SRP_{corr} was defined as $K_S sest$ (see "Seston P uptake kinetics"). Further, the theoretical time necessary for doubling of the actual epilithon P content – i.e.

402 epilithon phosphorus doubling time, *EPDT* (h) – was calculated applying the estimated P
403 uptake velocity:

404 $$EPDT = EPC/EPUV. \quad (8)$$

405 In eq. 8, *EPC* (µg P g OM^{-1}) is epilithon phosphorus content.

406

407 Abiotic P adsorption

408 To distinguish the P uptake by cells from the abiotic P adsorption, two samples with 4%
409 formaldehyde (final conc.) were pre-incubated overnight (>12 hours) in each experiment.
410 These samples received the lowest concentration of P_{add} used (i.e. 1 mg L^{-1}) and the effect of
411 formaldehyde was expressed relative to uninhibited uptake velocity. Additional experiments
412 were performed to elucidate concentration dependency of the abiotic adsorption over a
413 wide range of P concentrations (P_{add} = 0.01, 0.1, 1, and 10 mg P L^{-1}), and reversibility of the
414 abiotic P adsorption using the surface wash reagent[44,50] applied immediately after
415 termination of ^{33}P uptake experiments for 1 hour. The amount of ^{33}P released by the surface
416 wash reagent was expressed relative to the ^{33}P removed from the water in the presence of
417 4% formaldehyde.

418

419 Seston P uptake kinetics

420 Lake-water samples (30 mL) were supplemented simultaneously with 50–100 kBq of
421 carrier-free ^{33}P-labelled H_3PO_4 and seven concentrations of unlabelled orthophosphate (P_{add},
422 range 0.1–60 µg P L^{-1}, added as KH_2PO_4), and incubated at *in-situ* temperature for 2–3 hours.
423 At appropriate time intervals (2–30 min), 0.5-mL subsamples were filtered through
424 polycarbonate filters (Poretics, 0.2 µm mean porosity). The filter-retained activity was
425 measured with the scintillation counter. The P uptake rate constants, k_{upt}, were determined

426 from the time courses of ^{33}P incorporation with the method of Currie and Kalff[51] applying
427 the second-order polynomic equation:

428 $$P_t/T = P_0 + k_{upt} \times t + a \times t^2, \quad (9)$$

429 where P_t is filter-retained ^{33}P activity (c.p.m.) at time t, T is total ^{33}P activity added, and P_0 is
430 filter-retained ^{33}P activity at zero time, to the initial part of data ($P_t/T < 0.7$)[52]. The P uptake
431 velocity, v_{upt} (µg P L^{-1} h^{-1}) was calculated as:

432 $$v_{upt} = k_{upt} \times P_{add}\,. \quad (10)$$

433 The maximum velocity of P uptake, $V_{max}sest$ (µg P L^{-1} h^{-1}), and half-saturation constant,
434 K_Ssest, (µg P L^{-1}) were determined by non-linear regression as described above (Eq. 3). To
435 compare specific P uptake affinities of epilithon and seston, expressed in the same units, the
436 seston specific P uptake affinity, $SPUA_{sest}$ (L g OM^{-1} h^{-1}) was calculated as:

437 $$SPUA_{sest} = \frac{V_{max}sest}{K_Ssest \times OM}, \quad (11)$$

438 where *OM* is seston organic matter content (g L^{-1}) estimated from *Chla* concentration in lake
439 water assuming *OM:Chla* (w/w) ratio of 200[53]. Turnover time of dissolved orthophosphate,
440 TT-PO_4 (h), was determined as $1/k_{upt}$ measured in the absence of added P and used for
441 epilimnion P deficiency assessment[54].

References

1. Azim, M. E., Verdegem, M. C. J., van Dam, A. A. & Beveridge, M. C. M. *Periphyton: Ecology, Exploitation and Management*. (CABI, 2005).
2. Cantonati, M. & Lowe, R. L. Lake benthic algae: toward an understanding of their ecology. *Freshw. Sci.* **33**, 475–486 (2014).
3. Vymazal, J. & Richardson, C. J. Species composition, biomass, and nutrient content of periphyton in the Florida Everglades. *J. Phycol.* **31**, 343–354 (1995).
4. Wyatt, K. H. *et al.* Resource constraints highlight complex microbial interactions during lake biofilm development. *J. Ecol.* **107**, 2737–2746 (2019).
5. Dodds, W. The Role of Periphyton in Phosphorus Retention in Shallow Freshwater Aquatic Systems. *J. Phycol.* **39**, 840–849 (2003).
6. Vadeboncoeur, Y. & Steinman, A. D. Periphyton function in lake ecosystems. *Sci. World J.* **2**, 1449–1468 (2002).
7. Hudson, J. J., Taylor, W. D. & Schindler, D. W. Phosphate concentrations in lakes. *Nature* **406**, 54–56 (2000).
8. Grossman, A. R. & Aksoy, M. Algae in a Phosphorus-Limited Landscape. *Annu. Plant Rev. online* 337–374 (2018).
9. Tanaka, T. *et al.* Specific affinity for phosphate uptake and specific alkaline phosphatase activity as diagnostic tools for detecting phosphorus-limited phytoplankton and bacteria. *Estuaries and Coasts* **29**, 1226–1241 (2006).
10. Cáceres, C. *et al.* Temporal phosphate gradients reveal diverse acclimation responses in phytoplankton phosphate uptake. *ISME J.* **13**, 2834–2845 (2019).
11. Fitzsimons, M. F., Probert, I., Gaillard, F. & Rees, A. P. Dissolved organic phosphorus uptake by marine phytoplankton is enhanced by the presence of dissolved organic

nitrogen. *J. Exp. Mar. Bio. Ecol.* **530**, 151434 (2020).

12. Lindemann, C., Fiksen, Ø., Andersen, K. H. & Aksnes, D. L. Scaling Laws in Phytoplankton Nutrient Uptake Affinity. *Front. Mar. Sci.* **3**, 26 (2016).

13. Scinto, L. J. & Reddy, K. R. Biotic and abiotic uptake of phosphorus by periphyton in a subtropical freshwater wetland. *Aquat. Bot.* **77**, 203–222 (2003).

14. Hwang, S., Havens, K. E. & Steinman, A. D. Phosphorus kinetics of planktonic and benthic assemblages in a shallow subtropical lake. *Freshw. Biol.* **40**, 729–745 (1998).

15. Cembella, A. D., Antia, N. J. & Harrison, P. J. The Utilization of Inorganic and Organic Phosphorous Compounds as Nutrients by Eukaryotic Microalgae: A Multidisciplinary Perspective: Part I. *CRC Crit. Rev. Microbiol.* **10**, 317–391 (1984).

16. Taylor, W. D. & Lean, D. R. S. Phosphorus Pool Sizes and Fluxes in the Epilinnnion of a Mesotrophic Lake. *Can. J. Fish. Aquat. Sci.* **48**, 1293–1301 (1991).

17. Chen, F. & Taylor, W. D. A model of phosphorus cycling in the epilimnion of oligotrophic and mesotrophic lakes. *Ecol. Modell.* **222**, 1103–1111 (2011).

18. Healey, F. P. Slope of the Monod equation as an indicator of advantage in nutrient competition. *Microb. Ecol.* **5**, 281–286 (1980).

19. Button, D. K. Kinetics of nutrient-limited transport and microbial growth. *Microbiol. Rev.* **49**, 270–297 (1985).

20. Thingstad, T. F. & Rassoulzadegan, F. Conceptual models for the biogeochemical role of the photic zone microbial food web, with particular reference to the Mediterranean Sea. *Prog. Oceanogr.* **44**, 271–286 (1999).

21. Larondelle, N. & Haase, D. Valuing post-mining landscapes using an ecosystem services approach—An example from Germany. *Ecol. Indic.* **18**, 567–574 (2012).

22. European Commission. *A Clean Planet for All*. (EC, 2018).

23. Schultze, M., Pokrandt, K. H. & Hille, W. Pit lakes of the Central German lignite mining district: Creation, morphometry and water quality aspects. *Limnologica* **40**, 148–155 (2010).

24. Wolfe, J. E. & Lind, O. T. Phosphorus uptake and turnover by periphyton in the presence of suspended clays. *Limnology* **11**, 31–37 (2010).

25. Krumhardt, K. M. *et al.* Effects of phosphorus starvation versus limitation on the marine cyanobacterium Prochlorococcus MED4 I: uptake physiology. *Environ. Microbiol.* **15**, 2114–2128 (2013).

26. Hillebrand, H. & Sommer, U. The nutrient stoichiometry of benthic microalgal growth: Redfield proportions are optimal. *Limnol. Oceanogr.* **44**, 440–446 (1999).

27. Maberly, S. C., King, L., Dent, M. M., Jones, R. I. & Gibson, C. E. Nutrient limitation of phytoplankton and periphyton growth in upland lakes. *Freshw. Biol.* **47**, 2136–2152 (2002).

28. Liess, A., Drakare, S. & Kahlert, M. Atmospheric nitrogen-deposition may intensify phosphorus limitation of shallow epilithic periphyton in unproductive lakes. *Freshw. Biol.* **54**, 1759–1773 (2009).

29. Kahlert, M. C:N:P ratios of freshwater benthic algae. *Arch. Hydrobiol.,(Suppl.) (Advanc. Limnol.).* **51**, 105–114 (1998).

30. Frost, P., Elser, J. & Turner, M. Effects of Caddisfly Grazers on the Elemental Composition of Epilithon in a Boreal Lake. *J. North Am. Benthol. Soc.* **21**, 54–63 (2002).

31. Fitter, A. & Hillebrand, H. Microbial food web structure affects bottom-up effects and elemental stoichiometry in periphyton assemblages. *Limnol. Oceanogr.* **54**, 2183–2200 (2009).

32. Riber, H. H. & Wetzel, R. G. Boundary-layer and internal diffusion effects on

514 phosphorus fluxes in lake periphyton1. *Limnol. Oceanogr.* **32**, 1181–1194 (1987).
515 33. Kahlert, M., Hasselrot, A. T., Hillebrand, H. & Pettersson, K. Spatial and temporal
516 variation in the biomass and nutrient status of epilithic algae in Lake Erken, Sweden.
517 *Freshw. Biol.* **47**, 1191–1215 (2002).
518 34. Harrison, S. S. C. & Hildrew, A. A. G. Patterns in the epilithic community of a lake
519 littoral. *Freshw. Biol.* **39**, 477–492 (1998).
520 35. Danovaro, R. *et al.* Viriobenthos in freshwater and marine sediments: a review.
521 *Freshw. Biol.* **53**, 1186–1213 (2008).
522 36. Murphy, J. & Riley, J. P. A modified single solution method for the determination of
523 phosphate in natural waters. *Anal. Chim. Acta* **27**, 31–36 (1962).
524 37. Rigler, F. Radiobiological analysis of inorganic phosphorus in lakewater. *Int.*
525 *Vereinigung für Theor. und Angew. Limnol. Verhandlungen* **16**, 465–470 (1966).
526 38. Bentzen, E. & Taylor, W. D. Estimating Michaelis–Menten Parameters and Lake Water
527 Phosphate by the Rigler Bioassay: Importance of Fitting Technique, Plankton Size, and
528 Substrate Range. *Can. J. Fish. Aquat. Sci.* **48**, 73–83 (1991).
529 39. Tambi, H. *et al.* Relationship between phosphate affinities and cell size and shape in
530 various bacteria and phytoplankton. *Aquat. Microb. Ecol.* **57**, 311–320 (2009).
531 40. Larned, S. T., Nikora, V. I. & Biggs, B. J. F. Mass-transfer-limited nitrogen and
532 phosphorus uptake by stream periphyton: A conceptual model and experimental
533 evidence. *Limnol. Oceanogr.* **49**, 1992–2000 (2004).
534 41. Jackson, C. R., Churchill, P. F. & Roden, E. E. Successional changes in bacteral
535 assamblage structure during epilithic biofilm development. *Ecology* **82**, 555–566
536 (2001).
537 42. Mieczan, T. & Tarkowska-Kukuryk, M. Effect of substrate on periphyton communities

and relationships among food web components in shallow hypertrophic lake. *J. Limnol.* **71**, (2012).

43. Sañudo-Wilhelmy, S. A. *et al.* The impact of surface-adsorbed phosphorus on phytoplankton Redfield stoichiometry. *Nature* **432**, 897–901 (2004).

44. Yao, B. *et al.* A model and experimental study of phosphate uptake kinetics in algae: Considering surface adsorption and P-stress. *J. Environ. Sci.* **23**, 189–198 (2011).

45. ISO 10260:1992 Water quality — Measurement of biochemical parameters — Spectrometric determination of the chlorophyll-a concentration, Geneva, Switzerland. (1992).

46. Kopáček, J. & Hejzlar, J. Semi-micro determination of total phosphorus in freshwaters with perchloric acid digestion. *Int. J. Environ. Anal. Chem.* **53**, 173–183 (1993).

47. Mackereth, F. J. H., Talling, J. & Heron, J. F. *Water Analysis: Some Revised Methods for Limnologists*. *Freshwater Biological Association* (Freshwater Biological Association, 1978).

48. Procházková, L. Bestimmung der Nitrate im Wasser. *Fresenius' Zeitschrift für Anal. Chemie* **167**, 254–260 (1959).

49. Motulsky, H. J. & Brown, R. E. Detecting outliers when fitting data with nonlinear regression - A new method based on robust nonlinear regression and the false discovery rate. *BMC Bioinformatics* **7**, 123 (2006).

50. Tovar-Sanchez, A. *et al.* A trace metal clean reagent to remove surface-bound iron from marine phytoplankton. *Mar. Chem.* **82**, 91–99 (2003).

51. Currie, D. J. & Kalff, J. A comparison of the abilities of freshwater algae and bacteria to acquire and retain phosphorus. *Limnol. Oceanogr.* **29**, 298–310 (1984).

52. Currie, D. J. Phosphorus Deficiency and its Variation among Lakes. *Can. J. Fish. Aquat.*

562 *Sci.* **47**, 1077–1084 (1990).
563 53. Yacobi, Y. Z. & Zohary, T. Carbon:chlorophyll a ratio, assimilation numbers and
564 turnover times of Lake Kinneret phytoplankton. *Hydrobiologia* **639**, 185–196 (2010).
565 54. Istánovics, V., Pettersson, K., Pierson, D. & Duarte, R. Evaluation of phosphorus
566 deficiency indicators for summer phytoplankton in Lake Erken. *Limnol. Oceanogr.* **37**,
567 890–900 (1992).
568

Acknowledgements

This research was supported by grant No. 19-05791S funded by the Czech Science Foundation. Additional support was provided by the Czech Academy of Sciences within the internal program of the Strategy AV 21: Land save and recovery. The project would not be possible without tight cooperation with companies Palivový Kombinát Ústí s.p. and Sokolovská Uhelná, who provided a boat and chemical data.

Author contributions

E.K. and J.N. designed and performed experiments, interpreted results, and wrote the manuscript. K.C., P.Z., M.R., E.K., J.N. and K.R. performed field work. P.Z., P.C., K.C., K.R. and M.P. reviewed the early version of manuscript. P.C. analysed the data and made statistics. K.C. designed map of lakes and took photo of epilithon. P.Z. took aerial photos of the lakes (presented in Supplement). All authors reviewed and approved the final version of manuscript.

Additional Information

Competing Interests: The authors declare that they have no competing interests.

Supplementary Information is available for this paper at xxxxx

*Correspondence should be addressed to E.K. (eliska.konopacova@hbu.cas.cz).

Figures

Figure 1. Maps of the investigated post-mining lakes and location of the sampling sites (asterisks).

Figure 2. Biomass and elemental composition of epilithon in three post-mining lakes sampled in the Czech Republic in 2019. **(a)** epilithon dry weight and organic matter content expressed per overgrown area, **(b)** relationship between epilithon molar N:P and C:P molar ratios (error bars omitted for the sake of clarity), **(c)** epilithon C:N ratios. Columns show averages of 4 (2×2) values from two sampling sites and two depths ± SD. Different lowercase letters indicate significant seasonal differences within lakes ($p < 0.05$, Two-way ANOVA with Tukey's multiple comparisons post-test). Shaded areas (b, c) show values indicating P and N limitation, respectively, given by Hillebrand and Sommer[26].

Figure 3. Epilithon P uptake in three post-mining lakes sampled in the Czech Republic in 2019. **(a)** Abiotic P uptake (adsorption). Columns show averages of 4 values from two sampling sites and two depths ± SD**. (b)** Maximum P uptake capacity, V_{max}. **(c)** Half-saturation constant, K_S. Symbols in two lower panels show individual values. Different lowercase letters indicate significant seasonal differences within lakes ($p < 0.05$, Two-way ANOVA and Tukey's multiple comparisons post-test).

Figure 4. P uptake parameters of epilithon in three post-mining lakes sampled in the Czech Republic in 2019. **(a)** Epilithon specific phosphorus uptake affinity ($SPUA_E$), **(b)** calculated *in-situ* P uptake by epilithon. Symbols show individual values. Different lowercase letters indicate significant seasonal differences within lakes ($p < 0.05$, Two-way ANOVA and Tukey's multiple comparisons post-test).

Figure 5. Calculated epilithon internal P dynamics based on measured epilithon P uptake properties in three post-mining lakes sampled in the Czech Republic in 2019. **(a)** Epilithon phosphorus doubling time. Symbols show individual values; different lowercase letters indicate significant seasonal differences within lakes ($p < 0.05$; Two-way ANOVA and Tukey's multiple comparisons post-test), **(b)** comparison of observed (blue columns) and

theoretical (red columns) changes in epilithon P content. Columns show averages of 4 (2×2) values from two sampling sites and two depths ± SD.

Tables

Table 1. Chemical and limnological parameters of the three post-mining lakes in the Czech Republic sampled from the depth of 0.5 m at their deepest points in 2019. [1]Corrected *SRP* value - see Discussion for explanation, [2]mixed layer, [3]euphotic depth, the depth of 1% of the surface photosynthetically active radiation, [4]unstable stratification, [5]b.d.l. = below detection limit of 0.5 µg L^{-1} for *SRP*.

Table 2. Average values of epilithon biomass- and P uptake-related variables measured in three post-mining lakes in the Czech Republic in 2019. Differences were tested with two-way ANOVA with Lake and Sampling season as factors. [1]Different lowercase letters indicate significant difference between lakes or sampling seasons ($p < 0.05$; Tukey's multiple comparisons post-test), p is the significance of the difference (for full ANOVA table see **Supplementary Table 3**). [2]Data with variability exceeding one order of magnitude were log-transformed.

Table 3. A summary of estimates of kinetic parameters of P uptake by epilithon in three post-mining lakes in the Czech Republic in 2019 (parameters of Michaelis-Menten kinetics V_{max} and K_S, and specific P uptake affinity, $SPUA_E$) with indices of the goodness of fit. [1]N, S denote the North and South sampling site, respectively (see **Fig. 1** and **Supplementary Table 6**), [2]the most parsimonious model selected with F-test, MM - Michaelis-Menten kinetics (Eq. 3), L - linear model (Eq. 4), [3]best-fit parameter ± standard error of the estimate.

645 **Figure 1.**

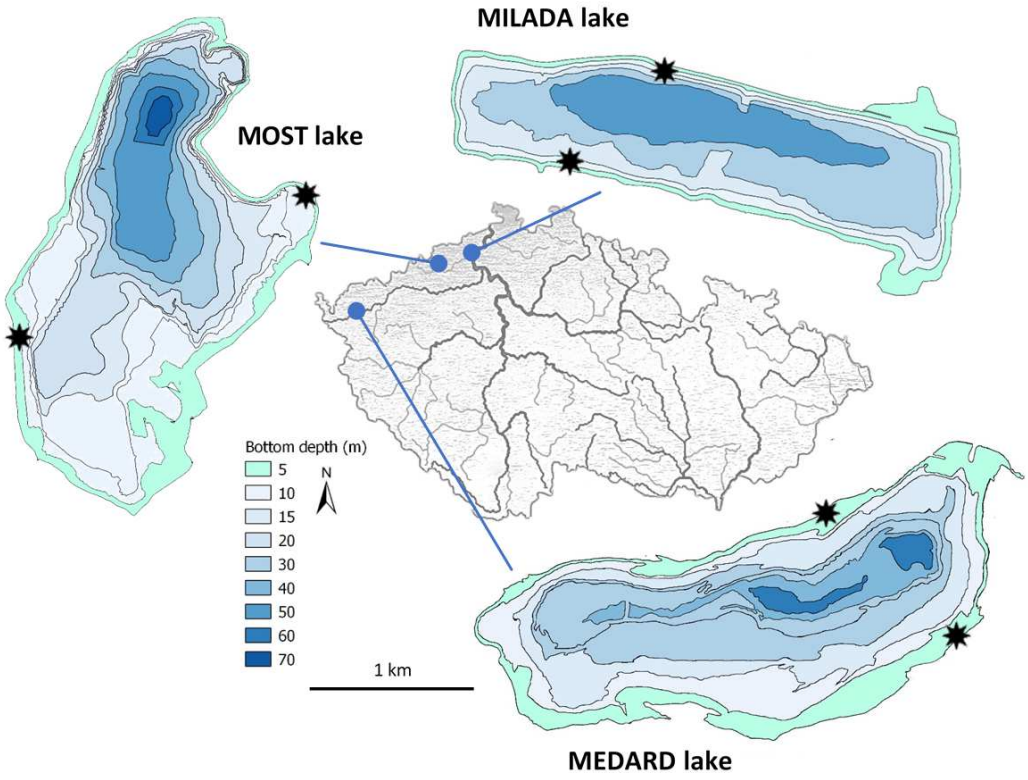

646

647

Figure 2.

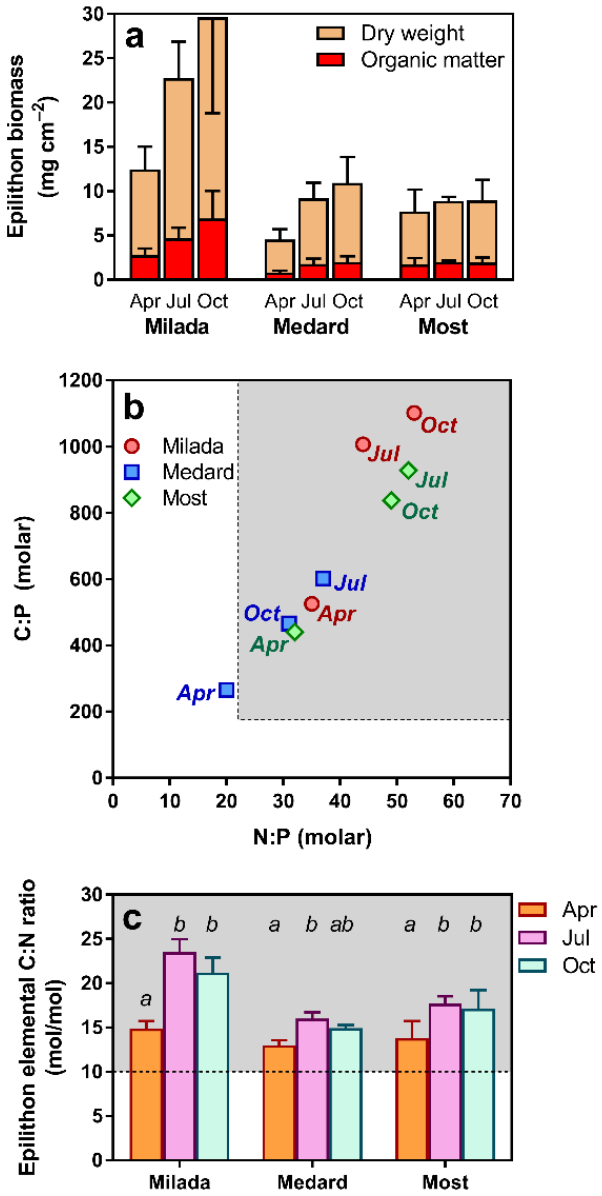
a
Dry weight
Organic matter
Epilithon biomass (mg cm^{-2})
Apr Jul Oct
Milada
Medard
Most
b
Milada
Medard
Most
C:P (molar)
N:P (molar)
c
Epilithon elemental C:N ratio (mol/mol)
Apr
Jul
Oct

650 **Figure 3.**

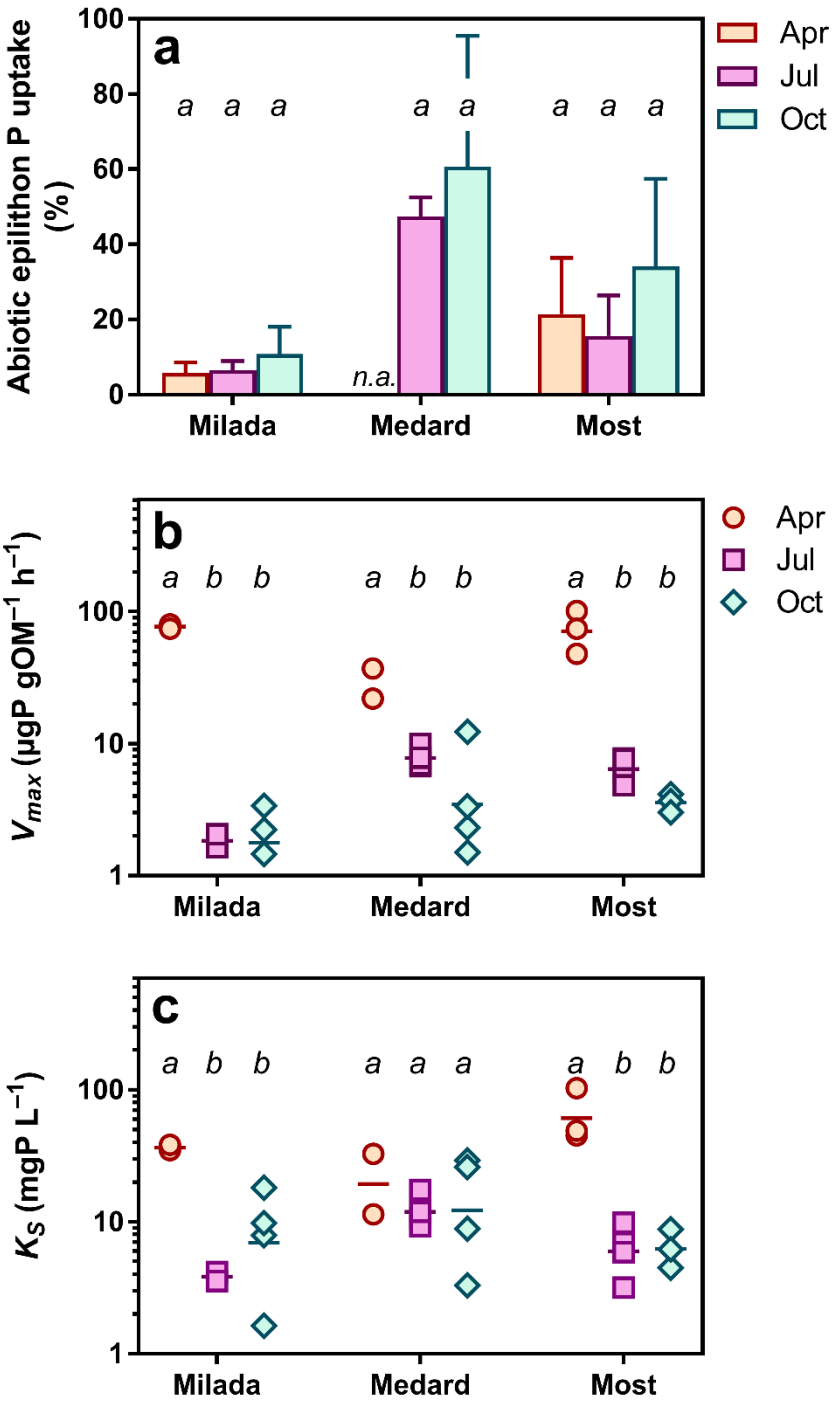

651

652 **Figure 4.**

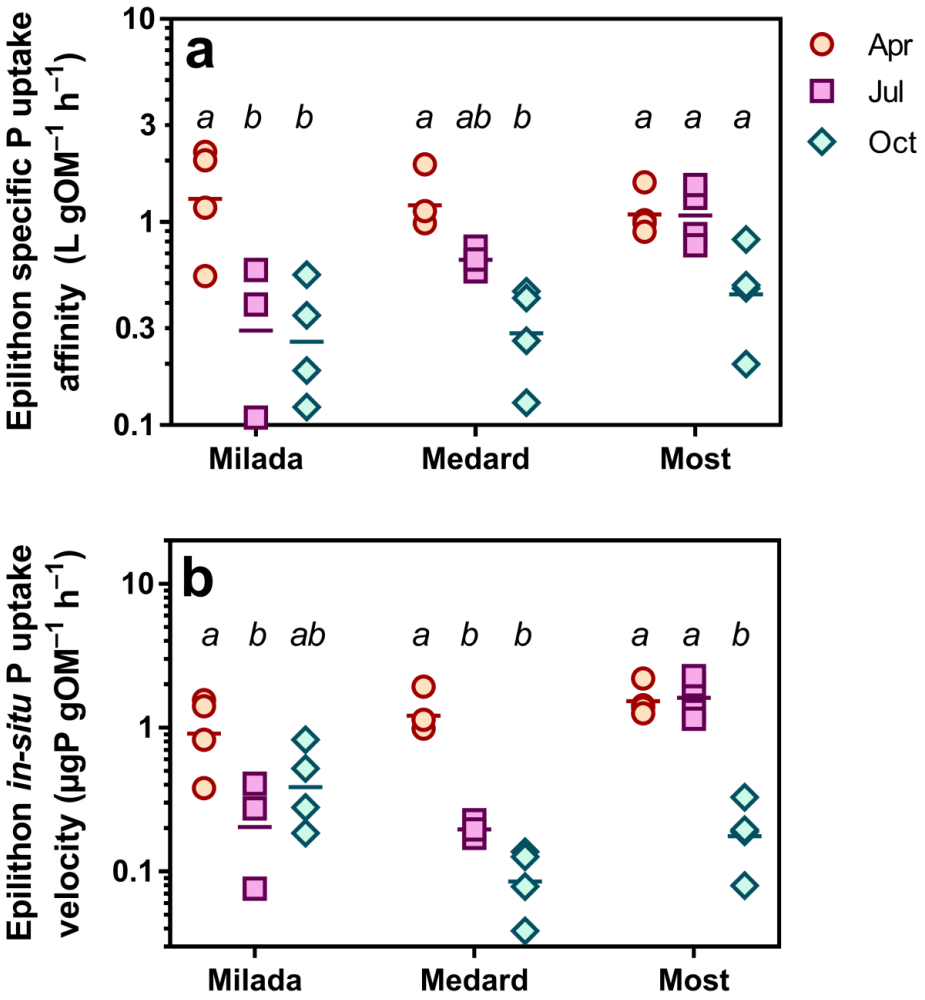

653

654 **Figure 5.**

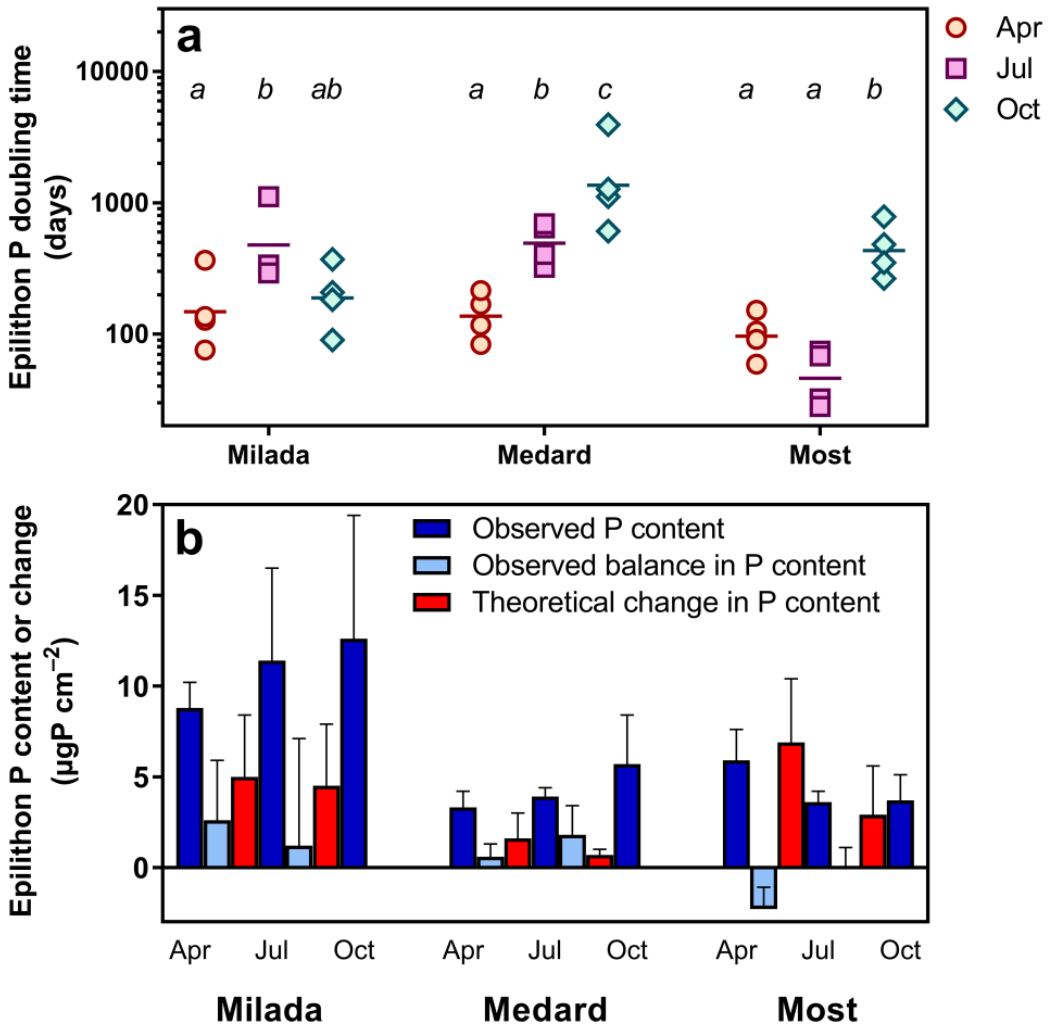

655

Tables

Table 1.

Lake	Month	T_w (°C)	pH	Conductivity (µS cm^{-1})	TP (µg L^{-1})	SRP (µg L^{-1})	SRP_{corr}[1] (µg L^{-1})	Si (mg L^{-1})	NO_3 (mg L^{-1})	DOC (mg L^{-1})	Chla (µg L^{-1})	Z_{mix}[2] (m)	Z_{eu}[3] (m)
Milada	April	7.7	9.1	1037	17.1	3.2	0.7	0.8	0.13	6.8	8.2	~8[4]	9.9
	July	22.4	9.1	1030	10.2	1.6	0.7	0.9	0.02	8.1	2.1	6	11.7
	October	14.8	9.1	1035	13.9	1.5	1.5	0.7	0.02	8.9	4.3	10	15.0
Medard	April	7.5	7.7	1093	4.5	1.0	1.0	2.7	1.26	3.0	0.6	~4[4]	9.4
	July	21.9	7.9	1080	4.0	b.d.l.[5]	0.3	2.9	1.12	3.1	1.0	7	17.6
	October	12.7	7.8	1087	4.0	b.d.l.	0.3	2.4	1.12	3.1	1.2	12	14.5
Most	April	11.7	8.6	540	7.9	1.6	1.4	1.2	0.92	4.6	1.0	5	16.7
	July	24.1	8.7	524	13.7	2.0	1.5	0.7	0.64	4.6	1.5	3	13.6
	October	17.0	8.8	533	14.2	2.1	0.4	0.5	0.56	5.0	3.1	10	14.6

Table 2.

	Lake averages[1]				Sampling-season averages[1]			
Epilithon variable	**Milada**	**Medard**	**Most**	**p**	**April**	**July**	**October**	**p**
Biomass (mg OM cm^{-2})	4.80^{a}	1.54^{b}	1.89^{b}	**<0.0001**	1.79^{a}	2.65^{ab}	3.63^{b}	**0.0042**
Biomass (mg DW cm^{-2})	16.7^{a}	6.7^{b}	6.6^{b}	**<0.0001**	6.4^{a}	10.1^{ab}	12.9^{b}	**0.0036**
OM/DW (%)	29^{a}	23^{b}	29^{a}	**0.0001**	27^{a}	26^{a}	28^{a}	0.5668
P content (mg P g OM^{-1})	2.49^{a}	3.14^{a}	2.42^{a}	0.058	3.64^{a}	2.21^{b}	2.18^{b}	**0.0001**
P content (µg P cm^{-2})	10.9^{a}	4.3^{b}	4.4^{b}	**<0.0001**	6.0^{a}	5.8^{a}	7.4^{a}	0.5314
C:P (molar ratio)	866^{a}	444^{b}	736^{a}	**0.0001**	411^{a}	831^{b}	802^{b}	**<0.0001**
C:N (molar ratio)	19.5^{a}	14.7^{b}	16.2^{c}	**<0.0001**	13.9^{a}	18.7^{b}	17.8^{b}	**<0.0001**
N:P (molar ratio)	43.8^{a}	29.4^{b}	44.4^{a}	**0.0086**	29.2^{a}	44.4^{b}	44.1^{b}	**0.0075**
V_{max} (mg P g OM^{-1} h^{-1})[2]	20.7^{a}	11.0^{ab}	26.0^{b}	**0.0446**	62.3^{a}	6.1^{b}	3.5^{c}	**<0.0001**
K_S (mg P L^{-1}) [2]	14.8^{a}	16.0^{a}	24.1^{a}	0.5495	44.8^{a}	8.3^{b}	11.3^{b}	**0.0002**
Specific P uptake affinity (L g OM^{-1} h^{-1}) [2]	0.75^{a}	0.74^{a}	0.91^{a}	0.0534	1.29^{a}	0.74^{b}	0.37^{c}	**<0.0001**
In-situ P uptake (µg P g OM^{-1} h^{-1})[2]	0.61^{ab}	0.52^{a}	1.15^{b}	**0.0002**	1.29^{a}	0.75^{b}	0.25^{c}	**<0.0001**
In-situ P uptake (µg P cm^{-2} d^{-1})[2]	0.058^{a}	0.013^{b}	0.054^{a}	**0.002**	0.054^{a}	0.041^{a}	0.029^{a}	0.1218
Doubling time of P in biomass (days) [2]	299^{a}	799^{b}	207^{c}	**<0.0001**	141^{a}	364^{a}	806^{b}	**<0.0001**

Table 3.

Date	Lake	Site[1]	Depth (m)	Best model[2]	F-test P	R^2_{adj}	V_{max} (mg P g OM^{-1} h^{-1})	K_S (mg P L^{-1})	$SPUA_E$ (L g OM^{-1} h^{-1})
15 Apr 2019	Milada	N	0.5	L	0.1124	0.6572	–	–	1.18 ± 0.16[3]
15 Apr 2019	Milada	N	1.5	MM	0.0132	0.7805	77.4 ± 30.4[3]	34.9 ± 19.1[3]	2.22 ± 0.52
15 Apr 2019	Milada	S	0.5	L	>0.9999	0.7237	–	–	0.543 ± 0.073
15 Apr 2019	Milada	S	1.5	MM	0.0125	0.8451	76.8 ± 25.4	38.2 ± 17.4	2.01 ± 0.38
22 Jul 2019	Milada	N	0.5	MM	0.0006	0.7778	1.64 ± 0.31	4.17 ± 1.79	0.393 ± 0.117
22 Jul 2019	Milada	N	1.5	L	0.1096	-0.2178	–	–	0.109 ± 0.026
22 Jul 2019	Milada	S	0.5	MM	0.001	0.5423	2.07 ± 0.51	3.55 ± 1.88	0.582 ± 0.209
14 Oct 2019	Milada	N	0.5	MM	0.0078	0.5802	1.46 ± 0.6	7.88 ± 5.54	0.186 ± 0.074
14 Oct 2019	Milada	N	1.5	MM	0.004	0.7236	3.39 ± 0.92	9.8 ± 4.55	0.347 ± 0.094
14 Oct 2019	Milada	S	0.5	MM	0.0003	0.9506	2.23 ± 0.35	18.13 ± 4.25	0.123 ± 0.014
14 Oct 2019	Milada	S	1.5	MM	0.0001	0.7764	0.9 ± 0.11	1.63 ± 0.63	0.55 ± 0.164
08 Apr 2019	Medard	N	0.5	L	>0.9999	0.7264	–	–	0.987 ± 0.147
08 Apr 2019	Medard	N	1.5	MM	0.0018	0.9254	37 ± 8.4	32.6 ± 9.6	1.13 ± 0.12
08 Apr 2019	Medard	S	0.5	MM	0.0003	0.787	21.9 ± 4.6	11.4 ± 4.1	1.93 ± 0.41
08 Apr 2019	Medard	S	1.5	L	*no MM fit*	0.5267	–	–	0.99 ± 0.164
08 Jul 2019	Medard	N	0.5	MM	0.0052	0.8073	6.74 ± 1.56	10.58 ± 4.44	0.637 ± 0.162
08 Jul 2019	Medard	N	1.5	MM	0.0001	0.9759	9.95 ± 1.09	17.38 ± 3.06	0.572 ± 0.051
08 Jul 2019	Medard	S	0.5	MM	<0.0001	0.944	6.98 ± 0.68	9.23 ± 1.56	0.757 ± 0.076

667 **Table 3.** *(cont.)*

Date	**Lake**	**Site**[1]	**Depth** (m)	**Best model**[2]	**F-test** p	$\mathbf{R^2_{adj}}$	V_{max} (mg P g OM^{-1} h^{-1})	K_S (mg P L^{-1})	$SPUA_E$ (L g OM^{-1} h^{-1})
21 Oct 2019	Medard	N	0.5	MM	0.0099	0.4554	2.32 ± 0.95	8.87 ± 6.6	0.261 ± 0.122
21 Oct 2019	Medard	N	1.5	MM	0.016	0.4669	1.51 ± 0.55	3.3 ± 2.62	0.456 ± 0.249
21 Oct 2019	Medard	S	0.5	MM	0.0145	0.7797	12.3 ± 4.4	29.1 ± 15.1	0.422 ± 0.099
21 Oct 2019	Medard	S	1.5	MM	0.042	0.6734	3.35 ± 1.57	25.9 ± 17.5	0.129 ± 0.04
29 Apr 2019	Most	N	0.5	MM	0.0217	0.8198	47.7 ± 19.1	46.7 ± 25	1.02 ± 0.21
29 Apr 2019	Most	N	1.5	MM	0.0116	0.9177	101 ± 33	103 ± 41	0.987 ± 0.11
29 Apr 2019	Most	S	0.5	L	0.1388	0.9414	–	–	0.897 ± 0.063
29 Apr 2019	Most	S	1.5	MM	0.0024	0.9074	73.9 ± 18.7	47 ± 15.4	1.57 ± 0.19
29 Jul 2019	Most	N	0.5	MM	0.0017	0.6322	6.04 ± 1.69	6.92 ± 3.59	0.872 ± 0.285
29 Jul 2019	Most	N	1.5	MM	0.0002	0.6232	7.73 ± 1.40	5.87 ± 2.73	1.32 ± 0.44
29 Jul 2019	Most	S	0.5	MM	<0.0001	0.814	4.83 ± 0.70	3.17 ± 1.07	1.52 ± 0.37
29 Jul 2019	Most	S	1.5	MM	<0.0001	0.9743	7.55 ± 0.60	9.81 ± 1.53	0.77 ± 0.08
30 Sep 2019	Most	N	0.5	MM	0.0016	0.7205	4.14 ± 1.09	8.76 ± 4.04	0.473 ± 0.131
30 Sep 2019	Most	N	1.5	MM	0.0007	0.7974	3.68 ± 0.70	4.49 ± 1.7	0.821 ± 0.201
30 Sep 2019	Most	S	0.5	MM	0.0124	0.5693	3.01 ± 1.00	6.17 ± 4.1	0.488 ± 0.207
30 Sep 2019	Most	S	1.5	L	0.1015	-0.3157	–	–	0.2 ± 0.046

668

Figures

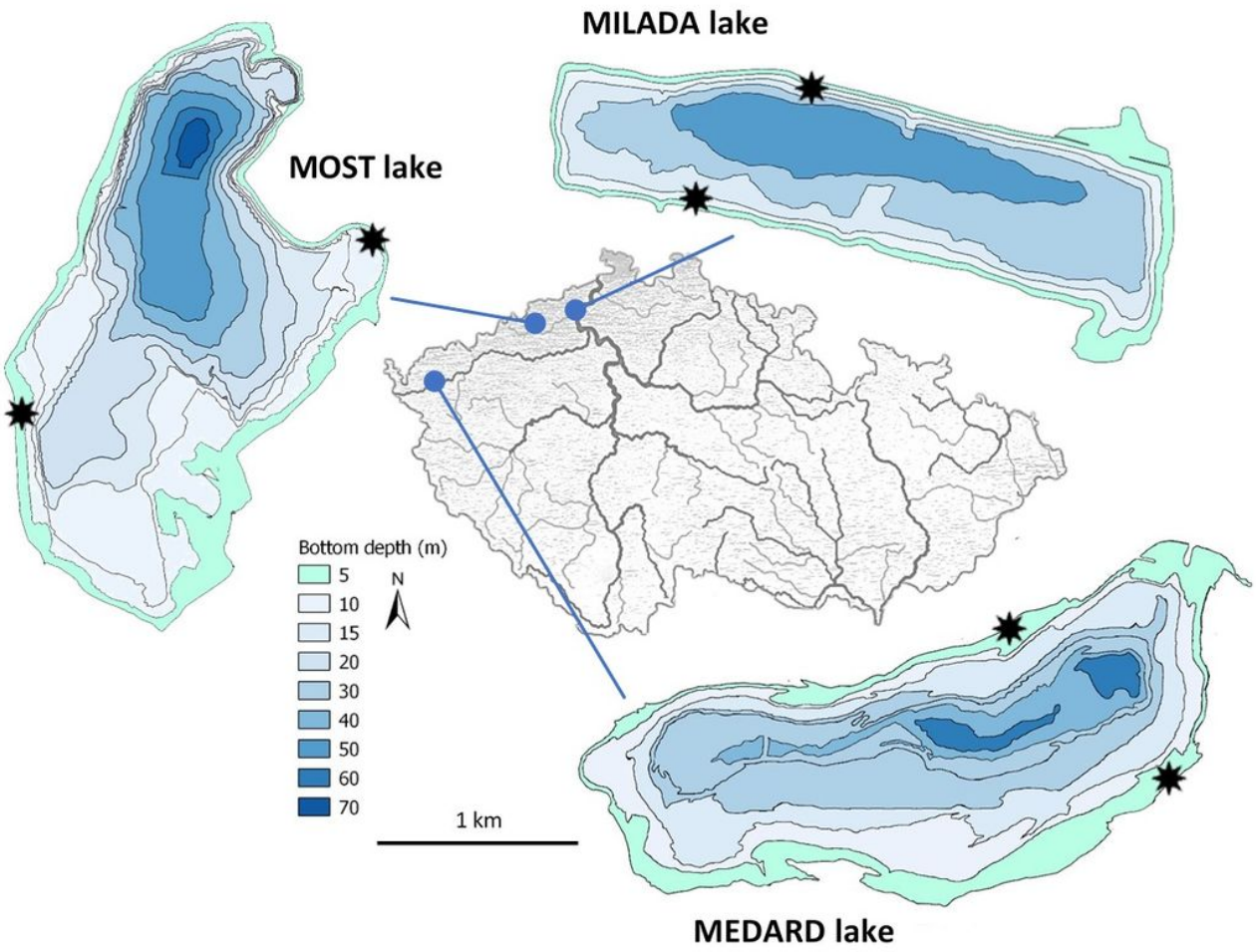

Figure 1

Maps of the investigated post-mining lakes and location of the sampling sites (asterisks).

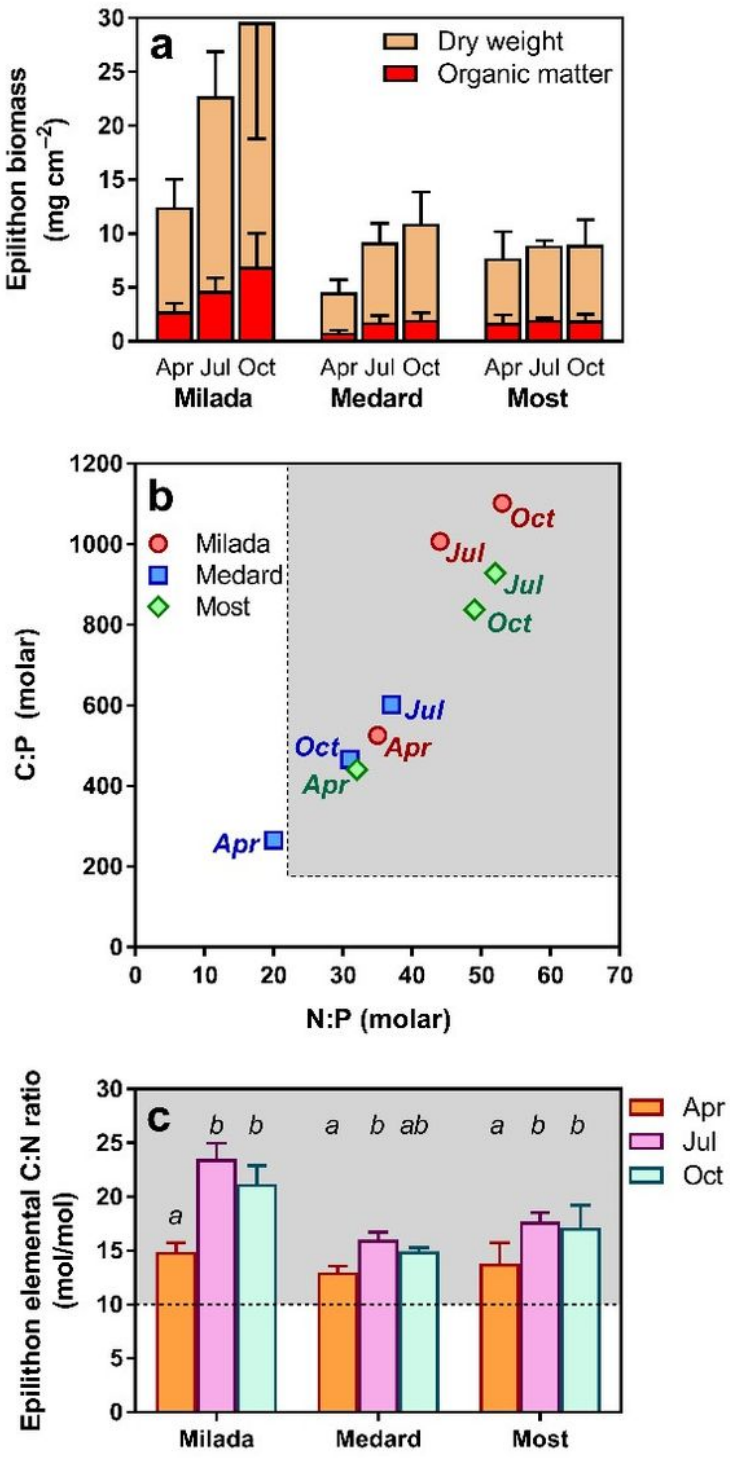

Figure 2

Biomass and elemental composition of epilithon in three post-mining lakes sampled in the Czech Republic in 2019. (a) epilithon dry weight and organic matter content expressed per overgrown area, (b) relationship between epilithon molar N:P and C:P molar ratios (error bars omitted for the sake of clarity), (c) epilithon C:N ratios. Columns show averages of 4 (2×2) values from two sampling sites and two depths ± SD. Different lowercase letters indicate significant seasonal differences within lakes ($p < 0.05$,

Two-way ANOVA with Tukey's multiple comparisons post-test). Shaded areas (b, c) show values indicating P and N limitation, respectively, given by Hillebrand and Sommer26.

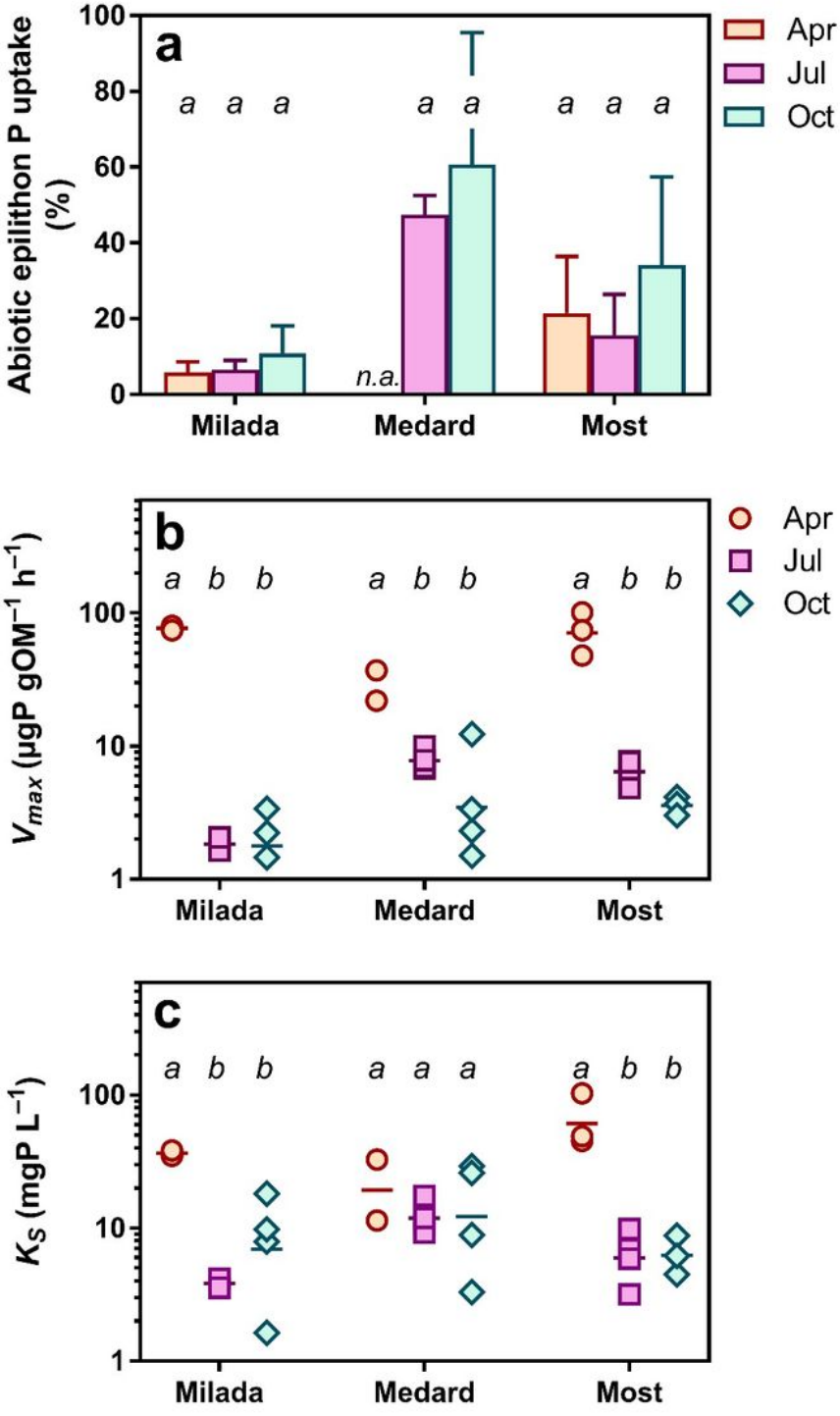

Figure 3

Epilithon P uptake in three post-mining lakes sampled in the Czech Republic in 2019. (a) Abiotic P uptake (adsorption). Columns show averages of 4 values from two sampling sites and two depths ± SD. (b) Maximum P uptake capacity, Vmax. (c) Half-saturation constant, KS. Symbols in two lower panels show

individual values. Different lowercase letters indicate significant seasonal differences within lakes ($p < 0.05$, Two-way ANOVA and Tukey's multiple comparisons post-test).

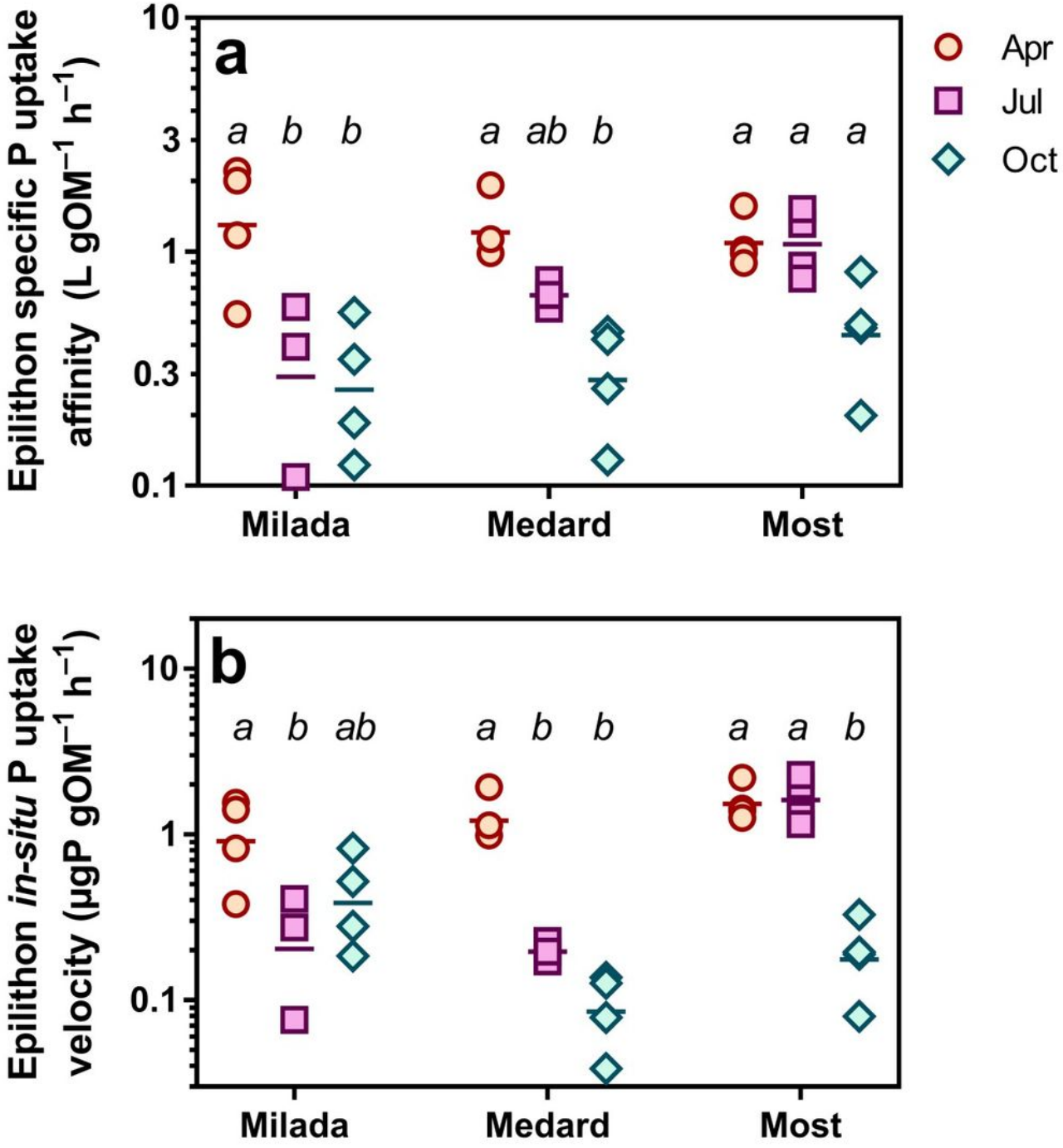

Figure 4

uptake parameters of epilithon in three post-mining lakes sampled in the Czech Republic in 2019. (a) Epilithon specific phosphorus uptake affinity (SPUAE), (b) calculated in-situ P uptake by epilithon.

Symbols show individual values. Different lowercase letters indicate significant seasonal differences within lakes ($p < 0.05$, Two-way ANOVA and Tukey's multiple comparisons post-test).

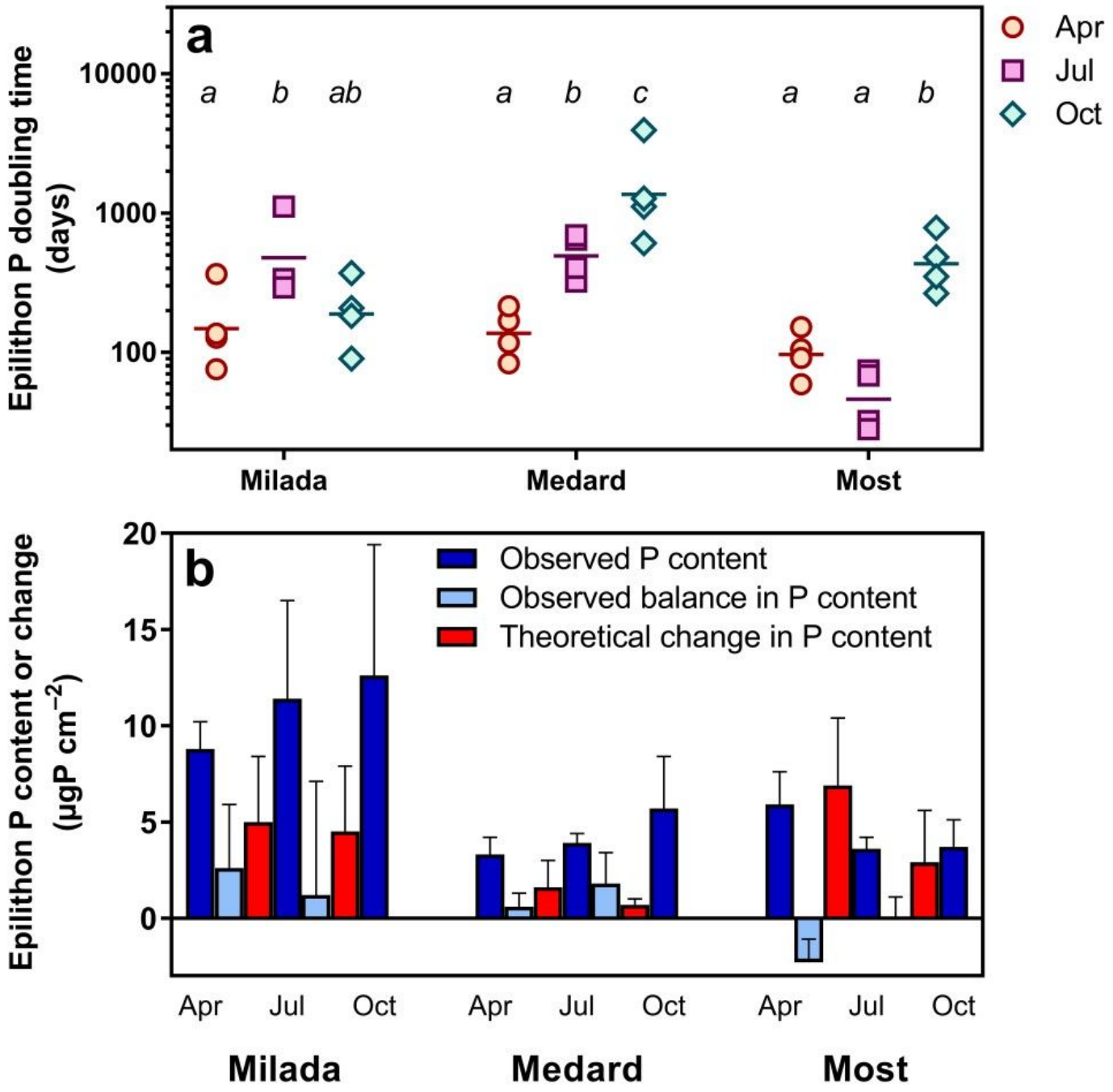

Figure 5

Calculated epilithon internal P dynamics based on measured epilithon P uptake properties in three post-mining lakes sampled in the Czech Republic in 2019. (a) Epilithon phosphorus doubling time. Symbols show individual values; different lowercase letters indicate significant seasonal differences within lakes ($p < 0.05$; Two-way ANOVA and Tukey's multiple comparisons post-test), (b) comparison of observed

(blue columns) and theoretical (red columns) changes in epilithon P content. Columns show averages of 4 (2×2) values from two sampling sites and two depths ± SD.

Supplementary Files

This is a list of supplementary files associated with this preprint. Click to download.

- EpilithonPuptakeKonopacovaSupplementaryTablesandFigures.pdf